

10-18-2004

# Ferroelectric nanomesa formation from polymer Langmuir-Blodgett films

Mengjun Bai

*University of Nebraska-Lincoln*, baime@missouri.edu

Stephen Ducharme

*University of Nebraska*, sducharme1@unl.edu

Follow this and additional works at: <http://digitalcommons.unl.edu/physicsducharme>



Part of the [Physics Commons](#)

---

Bai, Mengjun and Ducharme, Stephen, "Ferroelectric nanomesa formation from polymer Langmuir-Blodgett films" (2004). *Stephen Ducharme Publications*. 5.

<http://digitalcommons.unl.edu/physicsducharme/5>

This Article is brought to you for free and open access by the Research Papers in Physics and Astronomy at DigitalCommons@University of Nebraska - Lincoln. It has been accepted for inclusion in Stephen Ducharme Publications by an authorized administrator of DigitalCommons@University of Nebraska - Lincoln.

## Ferroelectric nanomesa formation from polymer Langmuir–Blodgett films

Mengjun Bai and Stephen Ducharme<sup>a)</sup>

*Department of Physics and Astronomy and Center for Materials Research and Analysis,  
University of Nebraska, Lincoln, Nebraska, 68588-0111*

(Received 5 April 2004; accepted 17 August 2004)

We report the fabrication and characterization of nanoscale ferroelectric structures consisting of disk-shaped nanomesas averaging  $8.7 \pm 0.4$  nm in height and  $95 \pm 22$  nm in diameter, and nanowells  $9.8 \pm 3.3$  nm in depth and  $128 \pm 37$  nm in diameter, formed from Langmuir–Blodgett films of vinylidene fluoride copolymers after annealing in the paraelectric phase. The nanomesas retain the ferroelectric properties of the bulk material and so may be suitable for use in high-density nonvolatile random-access memories, acoustic transducer arrays, or infrared imaging arrays. The nanomesa and nanowell patterns may provide useful templates for nanoscale molding or contact-printing. © 2004 American Institute of Physics. [DOI: 10.1063/1.1808251]

As the functional components of electronic and mechanical devices are reduced in the ongoing quest for smaller, faster, and cheaper technology, their performance may not scale with size due to the fundamentally different behavior of matter at the nanoscale, roughly 1–100 nm. Further, nanoscale structure can produce fundamentally new phenomena not evident or even possible in bulk materials. Nanoscale structuring of crystalline thin films can be accomplished by, e.g., lithographic patterning, self-assembly, aggregated growth, or melting followed by recrystallization. Here we report the spontaneous formation of highly crystalline ferroelectric nanomesas, measuring approximately 9 nm thick by 100 nm in diameter, from copolymer Langmuir–Blodgett films after annealing in the crystalline paraelectric phase. The results also show that the nanomesas retain stable ferroelectric properties, and that their formation in the paraelectric phase likely involves plastic crystalline flow, connected with conformational fluctuations.

Polyvinylidene fluoride (PVDF) and its copolymers with, e.g., trifluoroethylene (TrFE), are well-known crystalline ferroelectric materials,<sup>1–3</sup> which have a number of useful properties, such as piezoelectricity for use in electromechanical transducers,<sup>4,5</sup> or polarization bistability for use in nonvolatile memories.<sup>6,7</sup> The VDF copolymers typically crystallize from solution to form a jumble of crystalline lamellae with highly folded chains and dimensions of order 25 nm along the chains and 1–10  $\mu\text{m}$  perpendicular to the chains.<sup>1</sup> Annealing and drawing can improve crystallinity and microstructure, even to the point of producing highly oriented crystals with predominately straight chains.<sup>8</sup> Several recent studies have demonstrated stability of the polarization in nanometer-thick films fabricated by Langmuir–Blodgett (LB) deposition,<sup>9,10</sup> and the possibility of manipulating nanoscale domains with size 250 nm in a 75-nm-thick solvent-crystallized films of the 70:30 copolymer,<sup>11</sup> and 65 nm in 75-nm-thick evaporated films of VDF oligomers.<sup>12</sup>

The samples were fabricated from copolymers of vinylidene fluoride (VDF) with trifluoroethylene (TrFE) by horizontal (Schaefer) LB transfer to electronic-grade (100) silicon wafers, described in greater detail elsewhere.<sup>13</sup> To produce the nanowell and nanomesa patterns, the continuous

LB films were annealed in air at constant temperature, typically 125 °C, for 1 h, with heating and cooling rates of 1 °C per min. Samples for structural measurements were fabricated on silicon substrates. Capacitors for electrical measurements, were fabricated by first vacuum-coating a glass microscope slide with aluminum strip electrodes 1 mm wide and 20 nm thick, depositing and annealing the copolymer LB film, depositing a polyethylene LB film,<sup>14</sup> and topping with another set of aluminum electrodes oriented perpendicular to the bottom electrodes. The x-ray diffraction (XRD) data were obtained in the  $\theta$ – $2\theta$  geometry with a fixed Cu anode source (1.54 Å wavelength). Sample capacitance was measured with an impedance analyzer (HP 4192A) operating at 1 kHz with 0.1 V amplitude. The pyroelectric response of the capacitors, which is proportional to the net polarization,<sup>15</sup> was measured at zero bias by modulating the sample temperature with a 6 mW helium-neon laser beam modulated at 2 kHz, and recording the ac pyroelectric current from the sample with a lock-in amplifier.

Annealing the thinnest films results in the formation of nanoscale patterns. Figure 1(a) shows atomic force microscopy (AFM, Digital Instruments model Dimension 3100) images of progressively thicker films of P(VDF-TrFE 70:30), with molecular weight 100 000 g/mol (about 360 nm long) deposited on silicon and annealed at 125 °C. The AFM image of a 1 ML annealed film reveals an array of predominately disk-shaped nanomesas, with average thickness  $8.7 \pm 0.4$  nm and diameter  $95 \pm 22$  nm. Line scans shown below each image reveal that the nanomesas are level and flat, with steep sides, as shown schematically in Fig. 1(b). The 2-ML films have more, and slightly thicker, nanomesas, some joined into oblong and other extended shapes. The 3-ML films exhibit more joining, tending toward percolation, as the number of nanomesas increases. The 5-ML films are mostly filled in, leaving a complementary pattern of nanowells [Fig. 1(c)], with average thickness  $9.8 \pm 3.3$  nm and diameter  $128 \pm 37$  nm. Films of 8 ML and thicker, or those covered with a constraining layer, remain continuous after annealing under similar conditions.

The nanomesa and nanowell films are highly crystalline, as determined from the XRD peak at 19.7° (Fig. 2), which corresponds to a spacing of 0.45 nm, the (110) *d*-spacing of P(VDF-TrFE 70:30) routinely observed in the all-*trans* ferroelectric  $\beta$  phase.<sup>16</sup> The presence of the (110) peak at 20°, but

<sup>a)</sup>Electronic mail: sducharme1@unl.edu

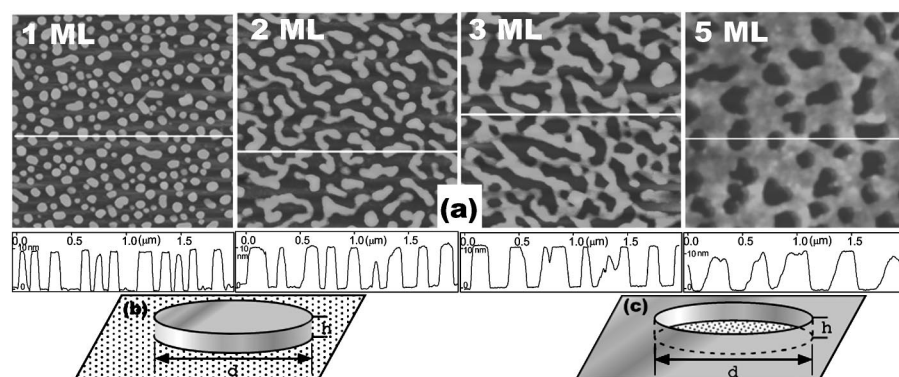


FIG. 1. (a) Atomic force microscope images of the nanomesa and nanowell formations in P(VDF-TrFE 70:30) LB films annealed at 125 °C for 1 h. Top row, left-right: 1, 2, 3, 5 ML films. Bottom row: corresponding AFM profiles recorded along the white line drawn on the images. The profile graphs have a 10 nm vertical scale. Idealized diagrams of the (b) nanomesa and (c) nanowell shapes.

not the (001) in-chain peak at 35°, shows that the chains are predominately parallel to the substrate. (The XRD data place an upper limit of 25% on the fraction of material with chains normal to the substrate.) The integrated intensity of the (110) peak increases rapidly with an increasing number of monolayers (Fig. 2 inset), due to the increased amount of material and the increased film thickness. The XRD peaks of the nanomesas are much stronger relative to the amount of polymer than that of a well-annealed continuous 20 ML film.

Remarkably, the nanomesas form only when annealed in the crystalline paraelectric phase, suggesting that the paraelectric phase exhibits significant plastic flow but the ferroelectric phase does not. This hypothesis is further supported by preliminary studies of low-temperature annealing, which revealed that the 75/25 and 50/50 copolymer LB films annealed in the phase coexistence region between the heating and cooling phase transition temperatures<sup>2,3</sup> did not form nanomesas, but did develop voids that increased in total area as the annealing temperature approached 110 °C. The increasing void area is consistent with the continuous conversion from the ferroelectric phase to the paraelectric phase as it is heated through the coexistence region.<sup>3</sup>

The spontaneous formation of nanomesas and nanowells in the ferroelectric polymer LB films is different from the usual mechanisms of crystalline film reorganization, melting and dislocation plasticity. First, the dimensions do not appear to be related to the size of the underlying molecular structures or to lamellar structures, but are influenced by substrate interactions and annealing temperature, indicating that surface energies play a major role. Second, the formation mechanism appears to involve crystalline plastic flow, not fluid flow, as the film restructuring occurs only in the crys-

talline paraelectric phase. Plastic deformation of crystalline polymers is usually associated with dislocations moving parallel to the polymer chains,<sup>17,18</sup> whereas the circular shape of the nanomesa belies a more isotropic process.

A kind of plastic crystal flow has been observed in the reorganization of polyethylene (PE)<sup>19</sup> and polyethylene oxide (PEO) lamellae<sup>20</sup> melted—or nearly melted—on a smooth substrate like silicon to produce structures resembling the nanowells (but not the nanomesas), with comparable thickness and diameter, but the crystalline structure is quite different. In the case of polyethylene lamellae, the thickness is determined by the chain segment length between folds, which is dependent on thermal history. Since the chains are parallel to the substrate in the case of the nanomesas, the thickness must be controlled by a different mechanism. In the case of PE, it has been suggested that the reorganization is preceded by melting, followed by recrystallization.<sup>19</sup> We confirmed that the LB films remained crystalline during annealing by monitoring the (110) XRD peak of the paraelectric *trans-gauche* phase,<sup>16</sup> though an initial melting and recrystallization occurring in the first few minutes would have been missed. Also, PVDF and its copolymers do not crystallize well from the melt.<sup>1</sup>

To understand plastic flow of the copolymers in the paraelectric phase, we need to look at the underlying mechanics of the polymer chains. The paraelectric phase is crystalline, a hexagonal close packing of linear chains consisting of alternating *trans-gauche* bonds, where the *gauche* bonds are randomly distributed between right- and left-hand sense.<sup>3,16</sup> The bond angles may fluctuate even far from the transition temperature.<sup>3,21</sup> Although the paraelectric phase is crystalline, the bond fluctuations<sup>16,22</sup> may provide enough free volume for plastic flow<sup>23</sup> necessary to reorganize the film.<sup>17,18</sup> This dynamical picture resembles the “condis” (conformational disorder) phase,<sup>23–26</sup> which would also explain the effectiveness of annealing VDF copolymers in the paraelectric phase, but not in the all-*trans* ferroelectric phase, which has a static all-*trans* conformation.<sup>3,16</sup>

The ferroelectric-paraelectric phase transition was evident in capacitance peaks at 63±3 °C on heating and 51±2 °C on cooling (Fig. 3), slightly lower than the peak temperatures typically observed in thicker continuous films and associated with the ferroelectric-paraelectric phase transition at 69±2 °C and the paraelectric-ferroelectric phase transition at 58±2 °C.<sup>3</sup>

Polarization switching was marked by capacitance peaks or by a change in sign of the pyroelectric response as the applied voltage was cycled (Fig. 4). The capacitance mea-

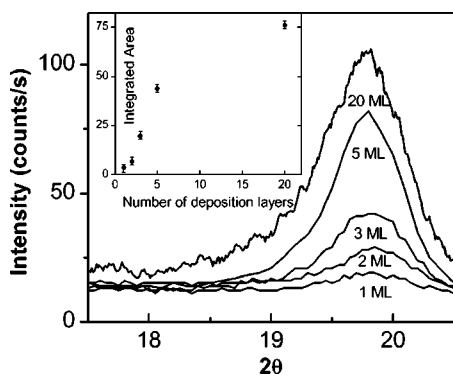


FIG. 2.  $\theta$ - $2\theta$  x-ray diffraction showing the (110) peaks from the 1, 2, 3, and 5 ML nanomesa films and a 20 ML continuous film. Inset: The dependence of the peak area on the number of layers.

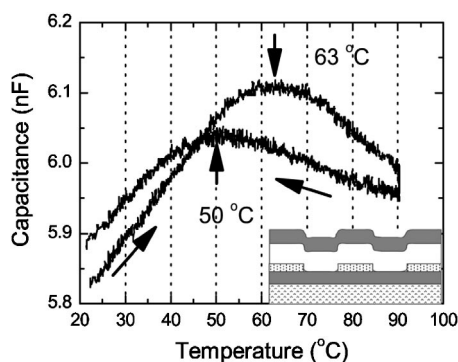


FIG. 3. Thermal hysteresis of the capacitance of a sample consisting of a 2 ML P(VDF-TrFE 50:50) nanomesa film, 1 ML polyethylene LB film, and aluminum electrodes. Inset: Profile of the nanomesa capacitor showing, from bottom to top, glass substrate, electrode, nanomesas, polyethylene LB film, and electrode.

measurements reveal the typical “butterfly” hysteresis shape<sup>10</sup> with peaks indicating polarization reversal and the pyroelectric hysteresis loop confirms the polarization reversal at approximately +14 and -13 V. The opposing polarization states were stable for at least 36 h at zero bias voltage. This shows that the nanomesas are stable against depolarization and formation of opposing domains, which is normally expected when there is a dielectric layer between the ferroelectric crystal and one or both electrodes (Fig. 3 inset) that prevents compensation charge from reaching the top surface. The nanomesa capacitors of the 50:50 copolymers exhibit similar dielectric and pyroelectric hysteresis, but capacitors consisting only of a 4 ML polyethylene LB film show no dielectric nonlinearity or hysteresis as the voltage is cycled over the same range.

The repeatable reversal of stable sample polarization evident in the pyroelectric and capacitance hysteresis (Fig. 4), plus the observation of repeatable dielectric anomalies

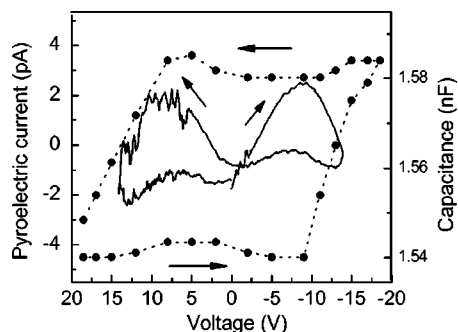


FIG. 4. Hysteresis at 25 °C in the capacitance and pyroelectric response of a capacitor consisting of a 3 ML nanomesa film and a 4 ML polyethylene LB film, with aluminum electrodes, like that shown in the inset to Fig. 3.

marking the phase transition between the ferroelectric and paraelectric phases (Fig. 3), confirm that the nanomesas are indeed ferroelectric, and that ferroelectricity is not significantly suppressed at nanoscale dimensions. Further study of the microstructure and formation dynamics of the nanomesas should reveal more about the complex static and dynamic interactions in the VDF copolymers responsible for ferroelectric order and plastic flow.

The authors thank Mitch Thompson of Measurement Specialties, Inc., for supplying VDF copolymer, Lan Gao, Kristin Kraemer, and Matt Poulsen for technical assistance, and Jiangyu Li and V. M. Fridkin for helpful discussions. This work was supported by the Nebraska Research Initiative and the National Science Foundation.

- <sup>1</sup>A. J. Lovinger, *Science* **220**, 1115 (1983).
- <sup>2</sup>T. Furukawa, *Phase Transitions* **18**, 143 (1989).
- <sup>3</sup>K. Tashiro, in *Ferroelectric Polymers*, edited by H. S. Nalwa (Dekker, New York, 1995), pp. 63–181.
- <sup>4</sup>H. Kawai, *Jpn. J. Appl. Phys.* **8**, 975 (1969).
- <sup>5</sup>*The Applications of Ferroelectric Polymers*, edited by T. T. Wang, J. M. Herbert, and A. M. Glass (Chapman and Hall, New York, 1988).
- <sup>6</sup>N. Yamauchi, *Jpn. J. Appl. Phys., Part 1* **25**, 590 (1986).
- <sup>7</sup>T. J. Reece, S. Ducharme, A. V. Sorokin, and M. Poulsen, *Appl. Phys. Lett.* **82**, 142 (2003).
- <sup>8</sup>H. Ohigashi, K. Omote, and T. Gomyo, *Appl. Phys. Lett.* **66**, 3281 (1995).
- <sup>9</sup>S. Palto, L. Blinov, A. Bune, E. Dubovik, V. Fridkin, N. Petukhova, K. Verkhovskaya, and S. Yudin, *Ferroelectr., Lett. Sect.* **19**, 65 (1995).
- <sup>10</sup>A. V. Bune, V. M. Fridkin, S. Ducharme, L. M. Blinov, S. P. Palto, A. V. Sorokin, S. G. Yudin, and A. Zlatkin, *Nature (London)* **391**, 874 (1998).
- <sup>11</sup>K. Kimura, K. Kobayashi, H. Yamada, T. Horiuchi, K. Ishida, and K. Matsushige, *Appl. Phys. Lett.* **82**, 4050 (2003).
- <sup>12</sup>K. Noda, K. Ishida, A. Kubono, T. Horiuchi, H. Yamada, and K. Matsushige, *Jpn. J. Appl. Phys., Part 1* **40**, 4361 (2001).
- <sup>13</sup>S. Ducharme, S. P. Palto, and V. M. Fridkin, in *Ferroelectric and Dielectric Thin Films*, edited by H. S. Nalwa (Academic, San Diego, 2002), Vol. 3.
- <sup>14</sup>A. V. Sorokin, M. Bai, S. Ducharme, and M. Poulsen, *J. Appl. Phys.* **92**, 5977 (2002).
- <sup>15</sup>A. V. Bune, C. Zhu, S. Ducharme, L. M. Blinov, V. M. Fridkin, S. P. Palto, N. N. Petukhova, and S. G. Yudin, *J. Appl. Phys.* **85**, 7869 (1999).
- <sup>16</sup>E. Bellet-Amalric and J. F. Legrand, *Eur. Phys. J. B* **3**, 225 (1998).
- <sup>17</sup>R. Séguéla, *J. Polym. Sci., Part B: Polym. Phys.* **40**, 593 (2002).
- <sup>18</sup>A. Flores, F. J. B. Calleja, and T. Asano, *J. Appl. Phys.* **90**, 6606 (2001).
- <sup>19</sup>P. H. Geil, *Polymer Single Crystals* (Interscience, New York, 1963).
- <sup>20</sup>G. Reiter, G. Castelein, and J.-U. Sommer, *Phys. Rev. Lett.* **86**, 5918 (2001).
- <sup>21</sup>J. F. Legrand, P. J. Schuele, V. H. Schmidt, and M. Minier, *Polymer* **26**, 1683 (1985).
- <sup>22</sup>A. J. Lovinger, *Macromolecules* **18**, 910 (1985).
- <sup>23</sup>H. Ohigashi, K. Omote, H. Abe, and K. Koga, *Jpn. J. Appl. Phys., Part 1* **68**, 1824 (1999).
- <sup>24</sup>B. Wunderlich and J. Grebowicz, in *Thermotropic Mesophases and Mesophase Transitions of Linear, Flexible Macromolecules* (Springer, Berlin, 1984), pp. 1–59.
- <sup>25</sup>G. Ungar, *Polymer* **34**, 2050 (1993).
- <sup>26</sup>M. Stock-Schweyer, B. Meurer, and G. Weill, *Polymer* **35**, 2072 (1994).